Intramolecular Donor–Acceptor Systems. Radiative and Nonradiative Processes for the Excited States of 2-*N*-Arylamino-6-naphthalenesulfonates

Edward M. Kosower,*[1a,b] Hanna Dodiuk,[1a] Kazutake Tanizawa,[1b] Michael Ottolenghi,[1c] and Naomi Orbach[1c]

Contribution from the Department of Chemistry, Tel-Aviv University, Ramat-Aviv, Tel-Aviv, Israel, the Department of Chemistry, State University of New York, Stony Brook, New York, 11790, and the Department of Physical Chemistry, Hebrew University, Jerusalem, Israel.
Received July 22, 1974

Abstract: 2-*N*-Arylamino-6-naphthalenesulfonates (ANS, **1**) are intramolecular donor–acceptor systems, in which the ground-state conformation of the *N*-aryl group is perpendicular (np = nonplanar) to the plane of the naphthalene ring. (1) The lowest energy electronic transitions of ANS derivatives are classified as $S_{0,np} \rightarrow S_{1,np}$ on the basis of the modest solvent and *N*-aryl substituent effects on the longest wavelength absorption band. (2) Two $S_1 \rightarrow S_0$ emissions are identified by different solvent and substituent effects on energies and quantum yields. Using the solvent polarity standard, $E_T(30)$ [more suitable in this case than *Z* value], and the substituent standard, the Hammett σ, the transitions are classified as (a) $S_{1,np} \rightarrow S_{0,np}$ (moderate solvent and substituent sensitivity) and (b) $S_{1,ct} \rightarrow S_{0,p}$ (ct = charge transfer, p $\simeq$ planar) (high solvent and substituent sensitivity). (3) Conversion of $S_{1,np}$ to $S_{1,ct}$ is an electron-transfer reaction which can be inhibited by substantial increases in solvent viscosity, e.g., using the polar solvent glycerol. (4) The fluorescence quenching in polar solvents is due to the conversion of $S_{1,ct}$ to S_0 by an electron-transfer reaction which is inhibited by a modest increase in solvent viscosity, e.g., in the polar solvent 1,2-ethanediol. (5) Three absorption bands can be observed for excited states generated by a laser pulse and are characterized by different maxima, lifetimes, and oxygen sensitivity: 810 nm, $\tau \sim 10$ nsec, O_2 insensitive (nonpolar: $S_{1,np} \rightarrow S_{n,np}$; polar: $S_{1,ct} \rightarrow S_{n,ct}$); 520 nm, $\tau \sim 5000$ nsec, O_2 sensitive ($T_{1,np} \rightarrow T_{n,np}$); 680 nm, $\tau \sim 300$ nsec, O_2 insensitive (CQ $\rightarrow$ CQ*, CQ = chemical quenching). (6) The $S_{1,np}$ origin for the triplet is confirmed by the intramolecular heavy-atom effects observed for halogenated ANS (**1**, X = F, Cl, Br). (7) Sterically hindered ANS derivatives (i.e., *N*-aryl = 2,6-dimethylphenyl) emit from both $S_{1,np}$ and $S_{1,ct}$ in fluid polar solvents. (8) A general scheme can be written to describe the radiative and nonradiative processes for intramolecular donor–acceptor systems like ANS derivatives as shown in Figure 13. (9) Results based on the use of ANS derivatives as "fluorescent probes" in biological systems may require reinterpretation.

2-*N*-Arylamino-6-naphthalenesulfonates (ANS, **1**) have the interesting property of fluorescing weakly in water and strongly in organic solvents or when bound to proteins. The discovery of these phenomena in 1954 by Weber and Laurence[2a] led to many studies designed to clarify the usefulness and the mechanism of this behavior, the most important being those of Stryer,[2b] McClure and Edelman,[3] Turner and Brand,[4] and Seliskar and Brand.[5] A key addition to the information collected by these groups was the finding by Kosower and Tanizawa[6] that two different light emissions from ANS could be distinguished on the basis of solvent effects. The effect of solvent polarity on the quenching of fluorescence, which is one of the essential points requiring a thorough explanation, was explained as due to intersystem crossing, even though no evidence concerning triplet formation was available. In the present work, we report both excited state emission and absorption studies which lead (with the aid of ground-state absorption data) to a new and fairly complete scheme for the radiative and nonradiative processes which account for the behavior of ANS derivatives. We shall see that the scheme extends our knowledge about excited-state systems[7a] to intramolecular donor–acceptor interactions which have been mainly investigated in intermolecular cases.

Previous studies by Chandross[7b] and Mataga[7c] have elucidated the weak geometric requirements for intramolecular exciplex formation without investigating the mechanism of quenching. Rates of formation of the charge-transfer state were thought to be shorter than the laser-pulse length used.[7c]

Results

Absorption Spectra ($S_0 \rightarrow S_1$). Absorption spectra for ANS derivatives exhibit only small changes for measurements in two solvents.[5] We have confirmed previous work on this point and have examined the longest wavelength transition in a little more detail since the upper state (S_1) is the origin of most of the processes we wish to consider. We have carefully looked for the maxima of the transition and, from the data assembled in Table I, can conclude that the solvent effect on the transition energy is small, and, in fact, is the opposite of what might be expected for a transition between a ground state with a modest dipole moment and an excited state with a high dipole moment. The Franck–Condon principle offers only a weak escape from this experimental finding since one of the potential charge carrying sites, the NH between the naphthalene and the aryl group, should be sufficiently solvated in the ground state to accommodate any extra charge which might accumulate in the excited state.

Changes in the substitution on the *N*-aryl group have little effect on the position of the long-wavelength absorption as shown by the data in Table I. The Hammett ρ value estimated for this process is -3.6, approximately what might have been predicted for an inductive effect like that on aniline basicity [$\rho(pK_a)$ for $ArNH_3^+$ dissociation is about 4.5]. From these data, we may infer that the *N*-aryl group is not conjugated with the aminonaphthalene system. From models and from studies on diphenylamine systems,[8,9] the equilibrium arrangement for the *N*-aryl group is no doubt approximately perpendicular to the plane of the naphthalene ring. The ground state may therefore be designated as $S_{0,np}$

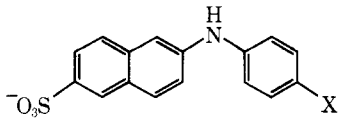

1

Table I. Solvent and Substituent Effect on Lowest Energy Absorption Band of 2-*N*-Arylamino-6-naphthalenesulfonate Derivatives

ANS (1) derivative, X =	Solvent	λ_{max},[a] nm	ϵ_{max}	ΔE_T[b]	m[b]
H	EtOH	358[c]	5300		
	H_2O	355	5100	0.68	0.045
CH_3	EtOH	360[c]	5600		
	H_2O	357	5000	0.67	0.045
CH_3O	EtOH	364[c]	4700		
	H_2O	359	4300	1.1	0.073
3-OCH_3[d]	EtOH	358[c]	6000		
	H_2O	355	5500	0.67	0.045
F	EtOH	360	4600		
	H_2O	355	4100	1.1	0.073
Br	EtOH	358	6300		
	H_2O	355	6100	0.67	0.045

[a] Resolved maximum. A smooth extension of the second maximum ($S_0 \rightarrow S_2$) was drawn and subtracted from the absorption curve in the region of the $S_0 \rightarrow S_1$ transition. On the basis of intensities, all observed absorptions are $\pi \rightarrow \pi^*$ in character. [b] Transition-energy difference between the absorption bands in ethanol and water is shown as ΔE_T. The magnitude of ΔE_T can be evaluated by comparison with the empirical solvent polarity standard Z, through the relation $\Delta E_T = m\Delta Z$ (Z values are discussed in E. M. Kosower, "An Introduction to Physical Organic Chemistry", Wiley, New York, N. Y., 1968). The m values for typical transitions are like those found for mesityl oxide, with $m(\pi \rightarrow \pi^*) = -0.18$ and $m(n \rightarrow \pi^*) = 0.15$ [E. M. Kosower, *J. Am. Chem. Soc.*, 80, 3261 (1958)]. [c] These maxima correspond to a ρ value of −3.6. The ρ value for the dissociation of anilinium ions in ethanol is 4.5. [d] *N*-Aryl = 3-methoxyphenyl.

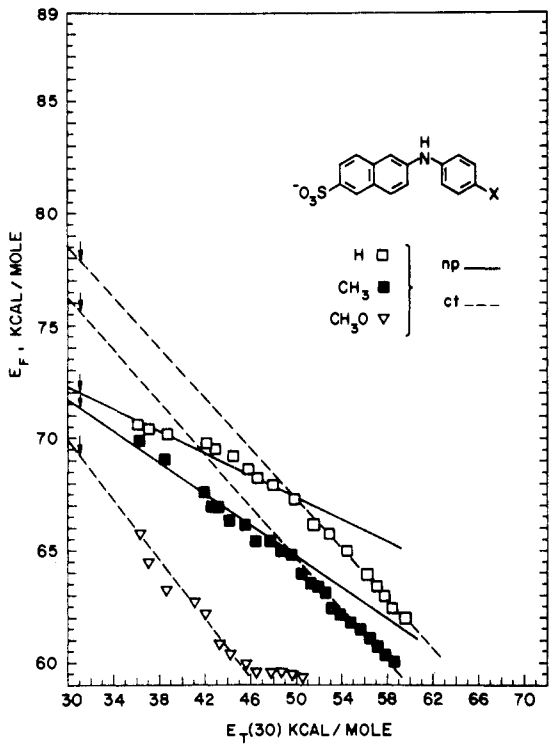

Figure 1. A plot of emission maxima (in kcal/mol) vs. the solvent-polarity parameter, $E_T(30)$ (in kcal/mol), for three 2-*N*-arylamino-6-naphthalenesulfonates (**1**, X = H, CH_3, CH_3O) in a series of dioxane–water mixtures. The solid line (——) correlates emissions assigned to the $S_{1,np}$ state and the dashed line (- - - -) emissions from the $S_{1,ct}$ state. The arrow indicates the location of the extrapolated values at $E_T(30) = 31.0$ (see Table VIII).

(np = nonplanar, indicating the nonplanar position of the *N*-aryl group with respect to the plane of the naphthalene ring) and the electronic transition corresponding to the longest wavelength absorption as $S_{0,np} \rightarrow S_{1,np}$. More precisely, we should write $S_{0,np} \rightarrow S^*_{1,np}$, the superscript referring to the nonrelaxed, vibrationally excited state (set of states) generated by the transition. We have shown elsewhere that there are observable photophysical consequences arising from the alteration in the relative rates of vibrational relaxation and intersystem crossing from $S^*_{1,np}$ at low temperatures.[10]

Emission Spectra ($S_1 \rightarrow S_0$). Previous work had demonstrated that the fluorescence maxima for ANS derivatives were strongly dependent on solvent polarity, emission energies moving to lower values for higher solvent polarities.[2,3] It was later shown that a variety of parameters associated with the fluorescence maxima (position, quantum yield, and band width) were correlated[5] with an empirical solvent polarity parameter, the Z value.[11] However, the authors chose to discuss the solvent sensitivity in terms of the quasimacroscopic Lippert-Mataga treatment.[12,13]

Careful examination of the published plots and rechecks using new data indicated that there might be two types of solvent sensitivity, one in nonpolar solvents and a second in polar solvents. We decided to try correlations of the fluorescence data with $E_T(30)$, an empirical solvent polarity parameter,[14] on three grounds: (a) availability of values for dioxane–water mixtures; (b) more appropriate model (intramolecular dipole annihilation);[15] and (c) good correlation with Z values.

Emission energies (from the fluorescence maxima) for three of the ANS derivatives (**1**, X = H, CH_3, OCH_3) in a series of dioxane–water mixtures are plotted against the corresponding $E_T(30)$ values in Figure 1. Data are given in Tables II, III, and IV. Two slopes are immediately apparent in the plots for the unsubstituted (**1**, X = H) and the methyl (**1**, X = CH_3) derivatives, the emission energies having a low sensitivity to solvent polarity change in the nonpolar range and a high sensitivity in the polar range. The high slope in the polar range (ca. 0.7) characterizes the emission as essentially charge transfer. The low slope in the nonpolar range (ca. 0.25) reflects only a modest difference in polarity between the excited state and ground state, with the excited state being the more polar. These rather different properties of the emitting states are best explained in terms of two different states. In the nonpolar range, the emitting state is termed $S_{1,np}$, in which np represents nonplanar as already defined. In the polar range, the state is labeled $S_{1,ct}$, in which ct describes the charge-transfer character of the emitting state.

The line in Figure 1 which represents data for the methoxy compound (**1**, X = OCH_3) has a slope which suggests that only emission from the $S_{1,ct}$ is being observed.

The quantum yields of fluorescence vary with solvent polarity in a way which is even more sensitive to the solvent polarity than the emission energies. In the nonpolar range, the quantum yield is usually fairly high in the least polar solvents and rises somewhat as polarity increases. At a solvent polarity value which depends on the particular ANS derivative, the quantum yield begins to drop rapidly and be-

Table II. Emission Data for 2-*N*-Arylamino-6-naphthalenesulfonates in Dioxane–Water Mixtures[a,b]

Solvent % dioxane–water[c]	$E_T(30)$ value[d]	Substituent (ANS, 1, X =): λ_{max}[e] (ϕ_F)[f]					
		CH_3	3-OCH_3	CH_3O	F	Cl	Br
99.9	36.3	409 (0.36)	405 (0.48)	435 (0.38)	404 (0.49)	399 (0.30)	396 (0.06)
99.6	37.0		407 (0.62)	443.5 (0.38)			
99.1	38.5	414 (0.43)		452 (0.27)	407 (0.60)	404 (0.40)	400 (0.08)
98.1	41.1		413 (0.67)	456 (0.27)		408 (0.39)	405 (0.07)
97.2	42.0	423 (0.44)	414.5 (0.66)	460 (0.20)	413 (0.63)	409 (0.42)	407 (0.08)
96.3	42.7	427 (0.38)					
95.3	43.2	427 (0.39)	418 (0.66)	470 (0.12)	416 (0.66)	411 (0.44)	409 (0.09)
94.4	44.2	431 (0.44)	420 (0.62)	473 (0.10)	419 (0.64)	413 (0.47)	410 (0.11)
92.5	45.6	432 (0.38)		477 (0.07)	420 (0.68)	415 (0.44)	413.5 (0.11)
90.6	46.5	437 (0.33)	423 (0.58)	480 (0.05)	421 (0.65)	417 (0.52)	415 (0.11)
85.9	47.8	437 (0.34)	424 (0.55)	480 (0.04)	422 (0.68)	417.5 (0.42)	416 (0.11)
81.3	48.7	440 (0.31)	424 (0.56)	480 (0.03)	423 (0.67)	418 (0.49)	417.5 (0.11)
76.6	49.7	441 (0.28)	426 (0.52)	481 (0.03)	424 (0.65)	418 (0.43)	418.5 (0.12)
71.9	50.5	447 (0.23)	428 (0.48)		426 (0.60)	420 (0.49)	419.5 (0.11)
67.2	51.3	450 (0.17)	432 (0.45)		428 (0.52)	422 (0.48)	421 (0.13)
62.5	52.0	451 (0.14)	435 (0.35)		432 (0.48)	425 (0.51)	422.5 (0.12)
57.8	52.6	453 (0.12)	438 (0.33)		435 (0.49)	427 (0.44)	424 (0.14)
53.1	53.2	458 (0.08)	440 (0.25)		439 (0.36)	429 (0.38)	427 (0.13)
48.4	53.9	460 (0.06)	444 (0.19)		443 (0.26)	431 (0.40)	430 (0.10)
43.2	54.9	463 (0.03)	448 (0.15)		446 (0.23)	435 (0.34)	434 (0.13)
39.1	55.8	465 (0.03)	453 (0.11)		448 (0.15)	439 (0.31)	437 (0.12)
34.4	56.5	468 (0.02)	458 (0.05)		451 (0.12)	443 (0.23)	440 (0.10)
29.7	57.2	471 (0.01)	461 (0.04)		455 (0.07)	449 (0.18)	449 (0.10)
25.3	57.9	474 (0.01)	465 (0.03)		459 (0.06)	454 (0.12)	456 (0.08)
20.3	58.7	476 (0.01)	472 (0.02)		465 (0.04)	459 (0.09)	461 (0.07)
11.0	60.9		471 (0.01)		470 (0.02)	470 (0.03)	466 (0.04)

[a] Temperature 25 ± 2°. Temperature effects on the position of the fluorescence maximum or the intensity of the emission over this temperature range are small. [b] For details of the measurement and the instrumentation, refer to the Experimental Section. [c] Percentage of dioxane by volume mixed with water. [d] Values were either taken from Table 2, p 28, in Ch. Reichardt and K. Dimroth, *Fortschr. Chem. Forsch.*, 11, 1 (1968) or derived from values in that table by linear interpolation. [e] In nm. [f] ±10% or less, according to reproducibility. Quinine sulfate in 0.1 *N* H_2SO_4, ϕ_F = 0.55.

Table III. Emission Data for 2-*N*-Phenylamino-6-naphthalenesulfonate in Dioxane–Water Mixtures[a]

Solvent % dioxane–water	$E_T(30)$ value	λ_{max} (ϕ_F)
100	36.1	405 (0.54)
99.6	37.1	406 (0.57)
99.0	38.6	407.5 (0.66)
97.1	42.1	410 (0.51)
96.1	42.9	411 (0.57)
94.1	44.4	413 (0.57)
92.1	45.8	416 (0.61)
90.2	46.6	419 (0.69)
85.3	47.9	421 (0.62)
75.4	49.9	425 (0.59)
65.6	51.5	432 (0.50)
55.7	52.9	435 (0.37)
45.9	54.4	440 (0.32)
36.1	56.2	447 (0.20)
31.2	57.0	451 (0.13)
26.2	57.7	454 (0.10)
21.3	58.4	458 (0.05)
16.4	59.5	461 (0.04)
6.6	61.8	465 (0.01)

[a] All footnotes of Table II apply.

Table IV. Emission Data for 2-*N*-(3,4-Methylenedioxyphenyl)-6-naphthalenesulfonate in Dioxane–Water[a]

Solvent % dioxane–water	$E_T(30)$ value	λ_{max} (ϕ_F)
100	36.0	451 (0.23)
99.7	37.0	454 (0.21)
99.1	38.4	466 (0.17)
98.2	40.8	475 (0.09)
97.4	41.9	479 (0.07)
95.6	42.8	486 (0.04)
94.7	43.9	491 (0.04)
92.9	45.2	495 (0.02)
91.2	46.2	497 (0.02)
86.8	47.6	500 (0.01)
82.4	48.5	497 (0.01)

[a] All footnotes of Table II apply.

comes so low in solvents as polar as water that it is difficult to measure accurately.

To illustrate the parallel behavior of both emission energy and quantum yield, data for the 3-methoxy derivative (**1**, X = 3- rather than 4-OCH_3) are plotted in Figure 2. Both the emission energy and quantum yield plots exhibit two slopes, the higher slope being found in the high polarity solvents.

In order to extend the range of substituents used, we examined a series of halogenated ANS derivatives (**1**, X = F, Cl, Br). The emission energies showed two-slope behavior when plotted as a function of solvent polarity for dioxane–water mixtures. The quantum yields also clearly showed two types of behavior in dioxane–water mixtures and revealed another novel feature of the behavior of ANS systems, one which we had already come across in the laser-photolysis studies to be described below. The emission from the $S_{1,np}$ state was decreased markedly by an intramolecular heavy-atom effect (promoting isc), whereas the emission from the $S_{1,ct}$ state was apparently unaffected. The failure to find a substantial heavy-atom effect on the $S_{1,ct}$ state does not exclude such an effect in principle but implies only that molecules like **1** undergo internal conversion from the $S_{1,ct}$ state faster than isc. It is important to note that the quantum yields for all of the halogenated ANS derivatives are approximately the same in glycerol (see below). The quantum yields as a function of solvent polarity for the three halogenated ANS derivatives are shown in Figure 3.

Since the relationship of the *N*-aryl group to the naphthalene ring was clearly of importance, we prepared a series of ANS derivatives in which steric hindrance to the rotation of the ring past the naphthalene ring would be hindered.

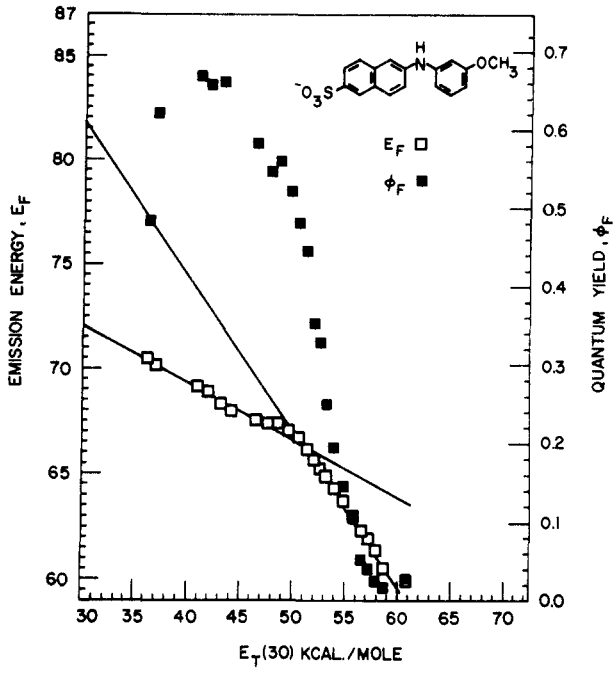

Figure 2. A plot of emission maxima (in kcal/mol) vs. the solvent-polarity parameter, $E_T(30)$ (in kcal/mol), derived from fluorescence spectra of 2-*N*-(3-methoxyphenyl)amino-6-naphthalenesulfonate in a series of dioxane–water mixtures. The linear extrapolations illustrated yield estimated emission maxima for the $S_{1,np}$ state in hydrocarbon [$E_T(30) = 31$], for the $S_{1,np}$ state in glycerol [$E_T(30) = 57.0$], and for the $S_{1,ct}$ state in hydrocarbon (see Table VIII).

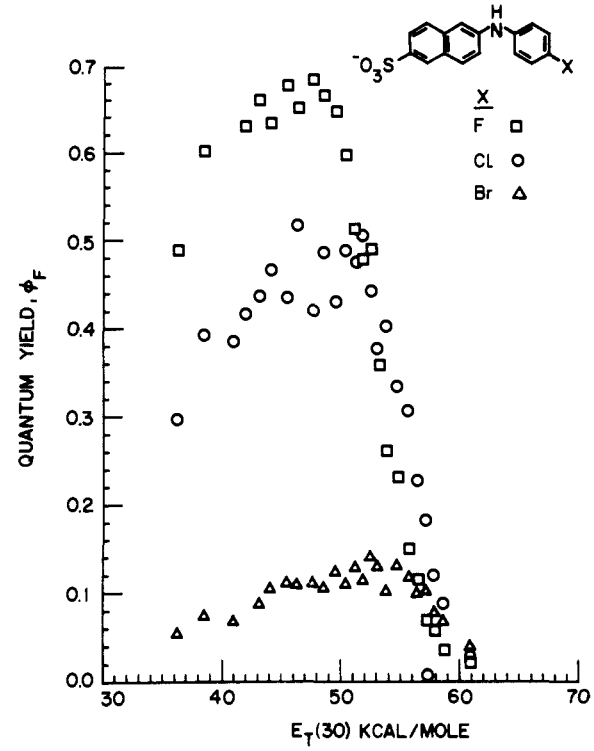

Figure 3. A plot of quantum yields for 2-*N*-(4-halophenyl)amino-6-naphthalenesulfonates vs. the solvent-polarity parameter, $E_T(30)$, based on fluorescence spectra measured in dioxane–water mixtures: (□) 4-fluoro; (○) 4-chloro; (△) 4-bromo.

Only one of these compounds, the 2,6-dimethyl derivative (**2**) will be considered at this time. A plot of emission energy against $E_T(30)$ yields a line which shows only a small change in slope at the point for which one might have expected the charge-transfer emission to appear. However, the quantum yield plot revealed precisely the type of behavior we had seen for almost all the other ANS derivatives (Figure 4). Emission data are listed in Table V. This apparent contradiction could be traced to the activity of both emitting states, $S_{1,np}$ and $S_{1,ct}$, the former dominating the emission. In Figure 5, the resolution of the fluorescence curve for **2** in 25% dioxane into two emission curves is given. Emission energies for the component assigned to the $S_{1,ct}$ state gives a good correlation (slope ca. 0.62) with $E_T(30)$, using data from dioxane–water mixtures containing between 43 and 11% dioxane (see Experimental Section).

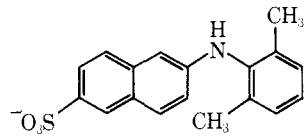

2

Emission data for all ANS derivatives in dioxane–water mixtures are summarized in Tables II, III, IV, and V.

The occurrence of two emitting states in a ratio dependent on solvent polarity and steric hindrance suggested that a more viscous medium than dioxane–water might be useful in lowering the rate of conversion of $S_{1,np}$ to $S_{1,ct}$. Previous workers had noted sharp increases in fluorescence quantum yield and changes in fluorescence maximum with an increase in viscosity.[3,5] Solvent relaxation within one excited-state manifold was assigned as the origin of viscosity induced changes in fluorescence emission maxima and quantum yields.[4] We have examined all of our ANS derivatives in glycerol and have also measured the $E_T(30)$ value for glycerol.[16] The observed maxima are listed in Table VI.

From the linear relationship of the emission energies and the solvent polarity values, we can estimate the emission energies to be expected in the solvent glycerol. The agreement between the maxima predicted for an $S_{1,np}$ emission

Table V. Emission Data for 2-*N*-(2,6-Dimethylphenyl)amino-6-naphthalenesulfonate in Dioxane–Water Mixtures[a]

Solvent % dioxane–water	$E_T(30)$ value	λ_{max} (ϕ_F)
100	36.3	395 (0.31)
99.6	37.0	396 (0.34)
99.1	38.5	397.5 (0.34)
98.1	41.1	399.5 (0.38)
97.2	42.0	400.5 (0.40)
96.3	42.7	401 (0.42)
95.3	43.2	402 (0.42)
94.4	44.2	403 (0.42)
92.5	45.6	404 (0.46)
90.6	46.5	404 (0.44)
85.9	47.8	405 (0.46)
81.3	48.7	406 (0.46)
76.6	49.7	406.5 (0.46)
71.9	50.5	407 (0.48)
67.2	51.3	407 (0.50)
62.5	52.0	407.5 (0.50)
57.8	52.6	408 (0.44)
53.1	53.2	409 (0.44)
48.4	53.9	410 (0.42)
43.2	54.9	412 (0.36)
39.1	55.8	413 (0.28)
34.4	56.5	415 (0.20)
29.7	57.2	416 (0.14)
25.3	57.9	417 (0.08)
20.3	58.7	418 (0.04)
10.9	60.9	419.5 (0.02)

[a] All footnotes of Table II apply.

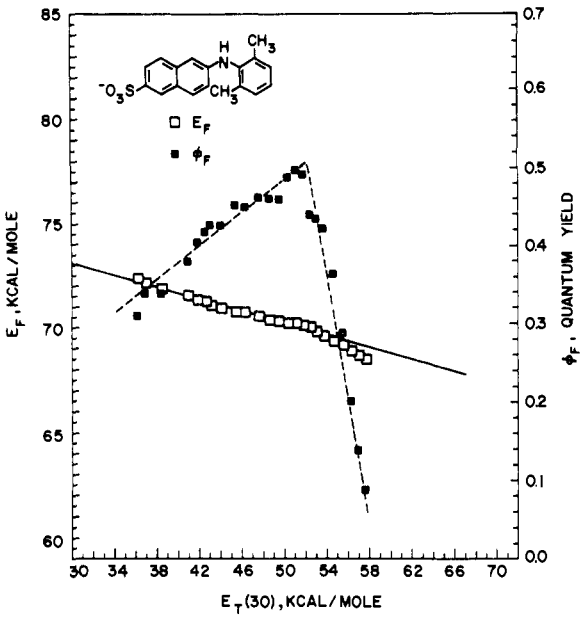

Figure 4. A plot of emission maxima (in kcal/mol) and quantum yields vs. the solvent-polarity parameter, $E_T(30)$ (in kcal/mol), for 2-*N*-(2,6-dimethylphenyl)amino-6-naphthalenesulfonate in a series of dioxane–water mixtures.

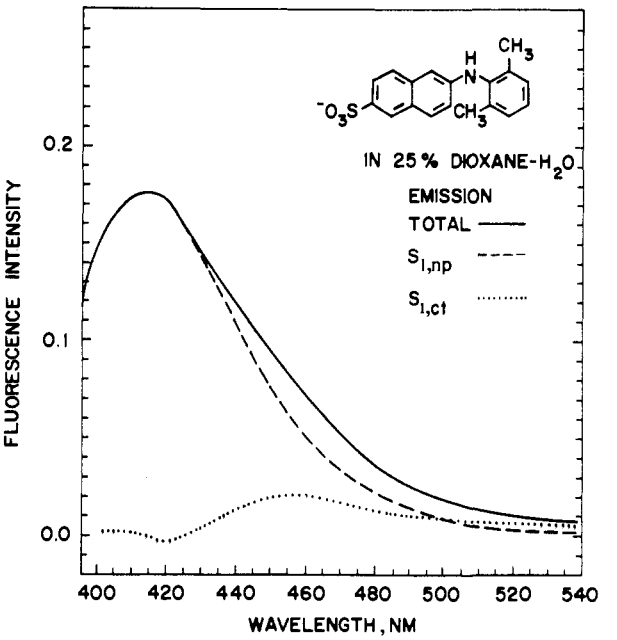

Figure 5. Resolution of fluorescence emission curve (——) for 2-*N*-(2,6-dimethylphenyl)amino-6-naphthalenesulfonate (2) in 25% dioxane–water into emission curves for the $S_{1,np}$ (- - - -) and $S_{1,ct}$ (. . . . .) states. (For details, see Experimental Section.)

Table VI. Fluorescence Data for ANS Derivatives in Glycerol

Compd 1, X =	Observed λ_{max} (nm)	Predicted λ_{max}[a] (nm)	Quantum yield, ϕ_F[b]
Br	436	433.2	0.43
Cl	430	432.5	0.47
F	437	438.4	0.43
H	437.5	436.2	0.49
CH_3	458	459.6	0.40
OCH_3	480	*c*	0.14
3-OCH_3[d]	439	441	0.49
3,4-OCH_2O[e]	492	*c*	0.04

[a] From the intersection of the linear correlation of emission energies classified as np and the vertical line for $E_T(30) = 57.0$ (measured value for glycerol). [b] By digital integration of the corrected spectrum and comparison with quinine sulfate in 0.1 *N* H_2SO_4 (ϕ_F = 0.55). Corrected for the refractive index of glycerol, ±0.04 or less. [c] The slope of the correlation line for the emission maxima in dioxane–water indicates that only charge-transfer emissions can be observed in solvents of low viscosity. [d] Substituent of 3 position of *N*-aryl group. [e] 3,4-Methylenedioxy substituent on *N*-aryl group.

and the observed maxima is reasonably good and confirms the emission in glycerol as $S_{1,np}$ in spite of the fact that the polarity of glycerol is much greater than needed to convert the $S_{1,np}$ to $S_{1,ct}$. The comparison of the predicted and observed maxima is shown in Table VI along with the quantum yields. The maxima are at much shorter wavelengths (higher in energy) than those found for an equivalent polarity in a solvent as fluid as dioxane–water.

Maxima could also be observed for several compounds which exhibited only charge-transfer emission in dioxane–water mixtures and for which no maximum could be observed in a dioxane–water solvent with a polarity equivalent to glycerol. In these cases (methoxy ANS, **1**, X = CH_3O and methylenedioxy-ANS, **1**, X = 3,4-OCH_2O–), the emission is assigned as $S_{1,np} \rightarrow S_{0,np}$.

Other results in solvents of moderate viscosity will be presented after we consider the data derived from laser-pulse photolysis.

Transient Absorption Spectra after Laser Pulse ($S_1 \rightarrow S_n$, $T_1 \rightarrow T_n$, CQ → CQ*). It was generally believed that intersystem crossing (isc) to the triplet from the initially formed excited singlet was responsible for the marked decrease in fluorescence of ANS derivatives in polar solvents. After the identification of the emitting state in polar solvents as $S_{1,ct}$, this explanation seemed even more plausible in view of the expected decrease in the singlet–triplet energy gap and the consequent increase in isc.[17] Nevertheless, in view of the central role of the phenomenon in the behavior and usefulness of ANS derivatives, a more definitive and direct study of the excited-state species was undertaken by means of laser-pulse photolysis.[18-20]

A number of the ANS derivatives were subjected to pulsed laser excitation in various dioxane–water mixtures and other solvents. At low water content (e.g., 95% dioxane), two transient changes in absorbance are detectable (Figure 11). A short-lived species with absorption peaking around 810 nm decays with a half-life of ~10 nsec, in agreement with the independently measured fluorescence decay. The absorbance left after the fast decay peaks around 510 nm and, in deaerated solutions, decays on the microsecond time scale. Aeration does not substantially affect the fast decay but reduces the lifetime of the 510-nm species to about 200 nsec.

After increasing the water content of deaerated ANS solutions, the laser pulse produces a third transient exhibiting a decay time of ~300 nsec with a maximum around 680 nm. Oxygen does not affect the behavior of the 680-nm species.

In view of the oxygen effect on the decay, and in consideration of the heavy-atom effect on the yield (see below), the 510-nm absorbance is readily attributable to the triplet state ($T_{1,np} \rightarrow T_{n,np}$). The 680-nm species, which does not represent an excited state, is denoted as CQ, designating a chemical quenching product. The 810-nm transient is assigned to the emitting S_1 state, its lifetime matching that of the fluorescence.

The relative yield of the triplet for the various ANS derivatives in different solvents was estimated from the absorbance change at 520 nm at 1000 nsec after pulsing [$OD(t_1)$]. At this time, both S_1 and CQ have decayed, and T_1 is the only absorbing species. The relative CQ yield was evaluated from the absorbance difference between absorb-

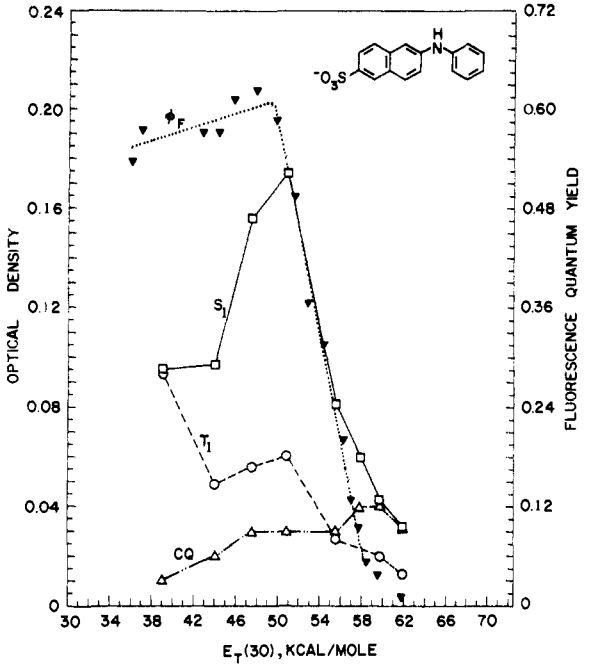

Figure 6. Plots of optical densities for light absorption by the excited states of 2-*N*-phenylamino-6-naphthalenesulfonate (**1**, X = H) and quantum yields vs. the solvent-polarity parameter, $E_T(30)$ (in kcal/mol), for a series of dioxane-water mixtures. The shortest lifetime absorption (either from $S_{1,np}$ or $S_{1,ct}$) is labeled S_1. The longest lived absorption (assigned to triplet, T_1) is so labeled, and the absorption from a species of intermediate lifetime is marked CQ. The quantum yields are indicated by filled triangles (▼). Data for the absorbance of S_1 are uncorrected for possible contributions of CQ and T_1 (see text).

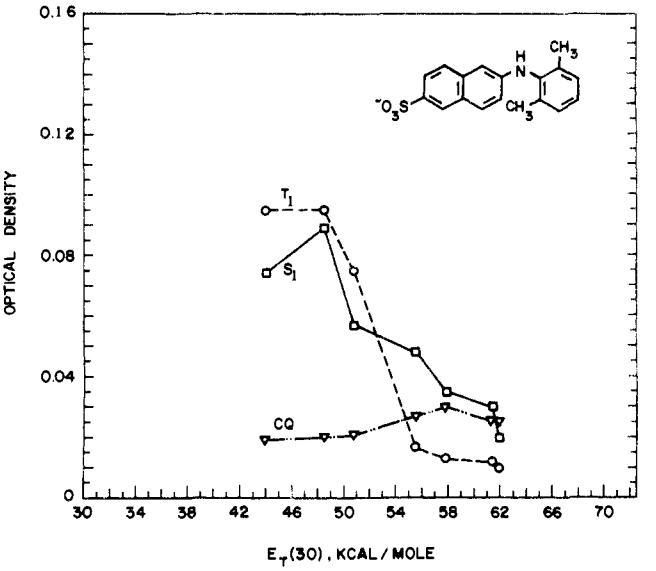

Figure 7. Plots of optical densities for light absorption by excited states of 2-*N*-(2,6-dimethylphenyl)amino-6-naphthalenesulfonate (**2**) vs. the solvent-polarity parameter, $E_T(30)$, in a series of dioxane-water mixtures. The labels, T_1, S_1, and CQ are explained in the caption for Figure 6. Data for the absorbance of S_1 are uncorrected for possible contributions from CQ and T_1 (see text).

ance at 70 and 100 nsec since CQ is the only species which changes on this time scale. For an exact evaluation of the contribution of S_1 to the absorbance at 10 nsec (especially at low total S_1 absorbance, as occurs in high polarity solvents), it is necessary to make arbitrary assumptions about the mechanisms which generate T_1 and CQ. Explicitly, if we assume that T_1 and CQ originate from S_1 in competition with fluorescence emission, they will reach their final absorbance values only after the complete decay of S_1. At 10 nsec, absorbance of T_1 and CQ will contribute only about 30% of their final absorbance. However, if formed in any prior process (e.g., by "fast" isc), their contribution could in principle be as high as 100% of their final absorbance. We have estimated the relative S_1 yield from the absorbance of S_1 at t = 10 nsec without making the corrections for the sake of simplicity. Corrections would improve still further the good correspondence between the quantum yield of fluorescence and the absorbance assigned to the S_1 state as illustrated in the plots for the optical densities for S_1, T_1, and CQ vs. $E_T(30)$ given in Figures 6-8. Figure 6 illustrates the behavior of the unsubstituted ANS including quantum yield (**1**, X = H), Figure 7 the 2,6-dimethyl derivative (**2**), and Figure 8 the bromo derivative (**1**, X = Br). Quantum yields for the solutions shown in Figures 7 and 8 are listed in Tables V and II, respectively.

Some general conclusions can be derived from the laser-pulse experiments. (a) Above a solvent polarity of $E_T(30)$ of $\simeq$ 50, the optical density assigned to S_1 exhibits a sharp drop matching that of the fluorescence quantum yield. (Corrections to the absorbance would improve the agreement.) In the low polarity range, from $E_T(30) \simeq 39$ to $E_T(30) \simeq 50$, both parameters increase. (b) In the high polarity range, absorbance of T_1 decreases in a fashion like that of S_1, implying that isc cannot explain the quenching of fluorescence found in polar solvents. (c) CQ is largely formed from $S_{1,ct}$ but also cannot be responsible for the quenching of fluorescence in polar solvents. There are two reasons for this conclusion: first, the formation of CQ does not parallel the decrease in fluorescence as the solvent becomes more polar; second, its quantum yield seems too low to explain a substantial change in fluorescence (unless CQ has an extraordinarily low absorption coefficient).

Through an examination of the potential-energy curves for the various states and the way in which they were likely to change with solvent, we considered an electron-transfer reaction from $S_{1,ct}$ to $S_{0,p}$ as the origin of the fluorescence quenching. This led to the experiments described in the next section.

Emission and Transient Laser Absorption Spectra in Solvents of Moderate Viscosity ($S_1 \rightarrow S_0$). If the return of $S_{1,ct}$ molecules to S_0 took place by way of a chemical reaction, we reasoned that the reaction might be subject to restrictions imposed by the rotations and solvent rearrangements required to produce the transition state. The success in inhibiting the $S_{1,np}$ to $S_{1,ct}$ conversion by a large increase in viscosity suggested that a more modest increase in viscosity might inhibit the $S_{1,ct}$ to S_0 reaction. The dramatic changes in the fluorescence quantum yield for a series of 1,2-ethanediol (ethylene glycol)-water mixtures confirmed this proposition and yielded a solid basis for understanding the fluorescence quenching reaction as an intramolecular electron-transfer reaction. A plot of emission maxima for 1,2 ethanediol-water mixtures is shown in Figure 9. The slope of the plot indicates quite clearly that the emissions are all from the $S_{1,ct}$ state. Even more impressive is the plot of quantum yield against solvent polarity shown in the same figure, especially when the plot is compared with the quantum-yield plot derived from dioxane-water mixtures [also shown in the figure]. In spite of the fact that the emission is being observed in a polar solvent, for which quenching might have been expected, there is a dramatic increase in the yield of fluorescence. The quantum yield in 1,2-ethanediol is about three times as high as it is in a dioxane-water solvent of equivalent $E_T(30)$ value.

Further studies of ANS in more viscous and less polar diols yielded parallel results; emission energies varied with solvent polarity as expected for charge-transfer transitions,

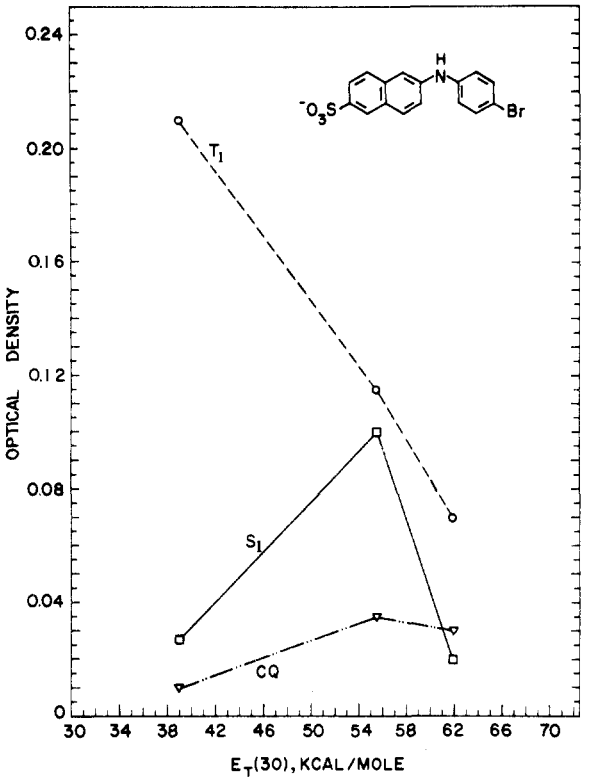

Figure 8. Plots of optical densities for light absorption by the excited states of 2-*N*-(4-bromophenyl)amino-6-naphthalenesulfonate (**1**, X = Br) vs. the solvent-polarity parameter, $E_T(30)$ (in kcal/mol), for a series of dioxane–water mixtures. The labels, S_1, T_1, and CQ are explained in the caption for Figure 6. Data for the absorbance of S_1 are uncorrected for possible contributions from CQ and T_1 (see text).

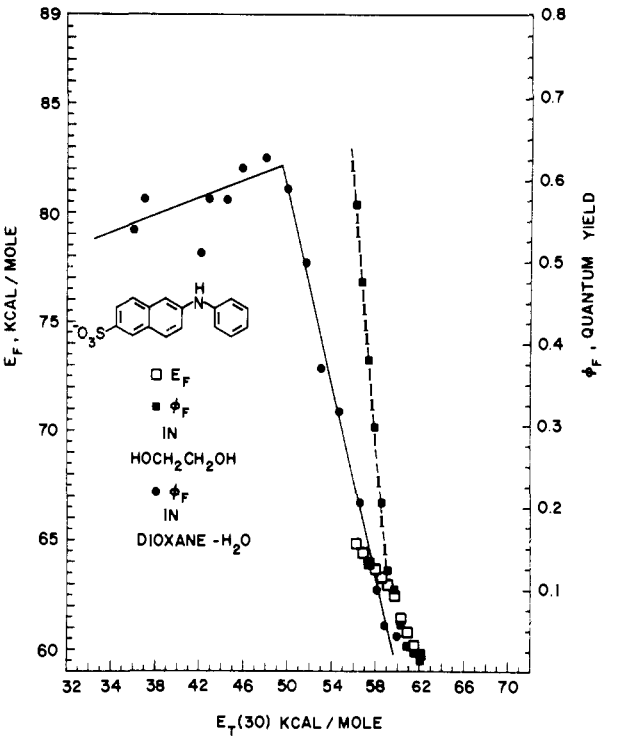

Figure 9. A plot of emission maxima (in kcal/mol) and quantum yields (- - - -) vs. the solvent-polarity parameter, $E_T(30)$ (in kcal/mol), for 2-*N*-phenylamino-6-naphthalenesulfonate (**1**, X = H) in a series of 1,2-ethanediol–water mixtures. The quantum-yield data for the same compound in dioxane–water mixtures as a function of solvent polarity (——) are included so that the substantial increases in the former solvent mixtures are more readily seen.

and quantum yields fell dramatically as water was added to the glycol solvent, reflecting an increase in polarity and a decrease in viscosity. The results for 1,2-ethanediol, 1,2-propanediol (Figure 10), and 1,3-propanediol are listed in Table VII.

Given the laser-pulse width (10 nsec),[21] it is clear that all or almost all $S_{1,np}$ will be converted to $S_{1,ct}$ (or will disappear by other routes) by the end of the pulse. The strong emission from $S_{1,ct}$ in 1,2-ethanediol indicated that the quenching pathway had been inhibited. It was thus of great interest to examine the transient absorption changes of the ANS in 1,2-ethanediol after a laser pulse. In complete agreement with the fluorescence data, it was found that the optical density for the absorbance assigned to S_1 was as high in 1,2-ethanediol [$E_T(30)$ = 56.3] as that observed in a much less polar solvent, a dioxane–water mixture with $E_T(30)$ = 52.

Discussion

The primary questions about the radiative and nonradiative processes of the excited state of ANS derivatives concern: (a) the evidence for two fluorescent states; (b) the nature of the process which converts one fluorescent state into the other; (c) the nature of the quenching in polar solvents; and (d) the role of intersystem crossing in the dynamics of the ANS system.

Two Fluorescent States. We have shown by means of a comparison between the energies of the fluorescent emission and a solvent-polarity parameter, $E_T(30)$, that ANS and its derivatives emit from two different states, the $S_{1,np}$ state and the $S_{1,ct}$ state. The plots by which the comparison was made can be further utilized to support the identification of the emitting states. The linear relationship between E_F and $E_T(30)$ can be extrapolated to hydrocarbon solvents to yield

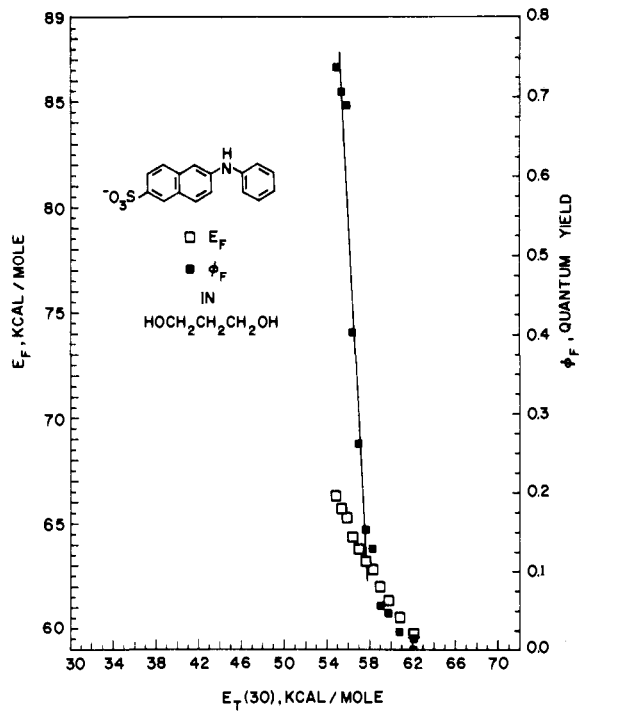

Figure 10. A plot of emission maxima (in kcal/mol) and quantum yields vs. the solvent-polarity parameter, $E_T(30)$ (in kcal/mol), for 2-*N*-phenylamino-6-naphthalenesulfonate (**1**, X = H) in 1,3-propanediol–water mixtures.

values for emission energies in solvents for which solvent interaction is minimal. We have chosen $E_T(30)$ = 31 as an appropriate solvent polarity value [$E_T(30)$ for *n*-hexane = 30.9] and have obtained values for the $S_{1,np}$ and $S_{1,ct}$ emission energies for all of the ANS derivatives. The lines

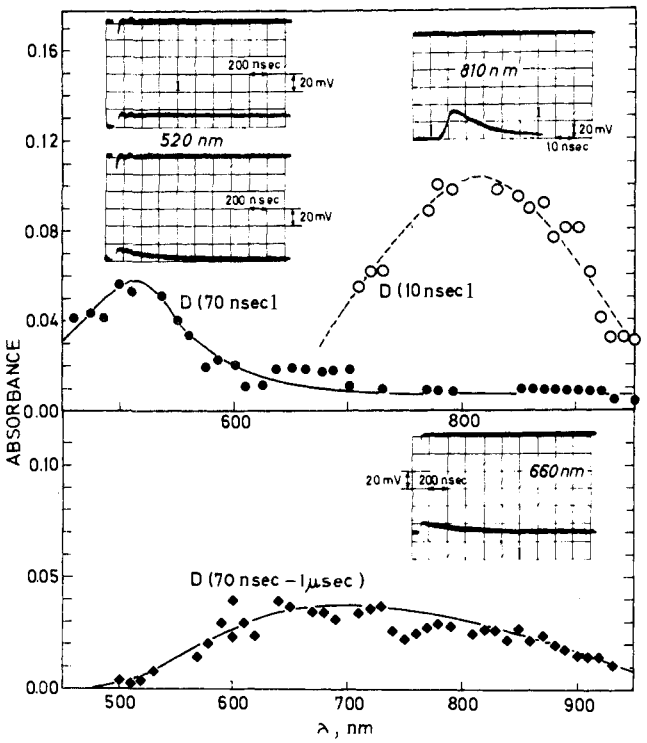

Figure 11. Characteristic oscillograms and transient spectra in the pulsed laser photolysis of $\sim 10^{-4}$ *M* ANS in dioxane–water mixtures. In each oscillogram, upper and lower traces are correspondingly recorded in the absence and in the presence of the monitoring light beam. (Top) Observations in 95% dioxane. The two oscillograms at 520 nm are in deaerated (upper) and aerated (lower) solutions. (Bottom) Observations in 25% dioxane.

drawn in Figures 1 and 2 illustrate the type of extrapolation which is involved. The lines can also be extrapolated to more polar solvents, and we have thus obtained predicted emission energies (E_F) for glycerol and diol solutions of ANS derivatives. The extrapolated emission energies are listed in Table VIII.

Processes with a small electron demand usually respond much less to substituents than processes with a high electron demand. In the case of ANS derivatives, *N*-aryl group substituents should contribute much less to the energy of the np emission than to the ct emission. We can express this conveniently in the form of a Hammett ρ value by correlating the extrapolated emission energies with Hammett substituent constants (σ). The correlations for both types of emissions are shown in Figure 12. The ρ value for the np emission is -2.8, a value consistent with an inductive effect on the excitation-induced migration of charge from the NH into the naphthalene ring. The ρ value for the ct emission is -10.2, a value so high as to strongly implicate charge transfer. Thus the substituent effect on the emissions leads to the same interpretation as that derived from solvent effects, with two different states being responsible for the fluorescence of ANS derivatives.

The σ constant for the 4-CH_3O group predicts a position for the extrapolated value of the np emission which is higher than that predicted for the ct emission correlated by σ^+ constants. Thus it is not surprising that 4-methoxy-ANS (**1**, X = CH_3O) gives rise to ct emissions in all dioxane–water mixtures. We can also estimate an approximate σ^+ constant for the 3,4-methylenedioxy group (3,4-OCH_2O-) as -0.97 from the extrapolated charge-transfer emission energy.

It is important to explicitly note that the twofold behavior of the emission with respect to energy and quantum yield as a function of solvent polarity establishes the two emitting states as distinct chemical species, rather than a single state which smoothly changes from a partially polarized to a fully polarized form.

Table VII. Emission Data for 2-*N*-Phenylamino-6-naphthalenesulfonate in Moderate Viscosity Solvents

Solvent % organic solvent–water[a]	$E_T(30)$,[b] kcal/mol	λ_{max}, nm	ϕ_F[d]
1,2-Ethanediol[c]			
100	56.3	441	0.57
91.4	56.9	444	0.48
82.9	57.5	447	0.38
74.3	58.1	449	0.20
65.7	58.6	452	0.21
57.1	59.2	454	0.12
48.6	59.8	458	0.10
40.0	60.4	465	0.06
31.4	61.0	470	0.03
22.9	61.6	475	0.02
14.3	62.1	479	0.01
1,2-Propanediol[c]			
100	54.0	430	0.59
90.6	54.7	436	0.74
81.3	55.4	440	0.54
71.9	56.1	443	0.45
62.5	56.7	446	0.35
53.1	57.3	450	0.21
43.2	58.1	454	0.10
34.4	58.6	461	0.06
25.3	59.2	469	0.03
15.6	60.3	476	0.02
6.3	62.0	482	0.01
1,3-Propanediol[c]			
100	54.9	431	0.74
90.6	55.4	435	0.70
81.3	55.9	438	0.69
71.9	56.5	444	0.40
62.5	57.0	448	0.26
53.1	57.7	452	0.15
43.2	58.4	455	0.13
34.4	59.0	461	0.06
25.3	59.8	466	0.05
15.6	60.9	472	0.02
6.3	62.2	478	0.01

[a] Percentage of diol by volume mixed with water. [b] Values were measured with the phenol betaine 30 according to Ch. Reichardt and K. Dimroth, *Justus Liebigs Ann. Chem.*, 661, 1 (1963). [c] Viscosity, 20° (in cP); 1,2 ethanediol, 20.9 (J. A. Monick, "Alcohols", Reinhold, New York, N.Y., 1968, p 312); 1,2-propanediol, 60.5 (p 315); 1,3-propanediol, 46.6 (ref 32, p 200); H_2O, 1.002 (D. Eisenberg and W. Kauzmann, "The Structure and Properties of Water", Oxford University Press, New York, N.Y., 1969, p 223). [d] See footnote *f*, Table II.

Table VIII. Extrapolated Values for $S_{1,ct}$ and $S_{1,np}$ Emissions in Hydrocarbon Solvent[a,b]

X	E_F(ct)[c]	σ_P^+	E_F(np)[d]	σ_P
Br	82.8	0.15	73.2	0.23
Cl	82.0	0.11	72.6	0.23
F	80.0	−0.07	72.1	0.06
H	78.0	0.00	72.0	0.00
CH_3	75.6	−0.31	71.3	−0.17
OCH_3	69.2	−0.78		−0.27
3-OCH_3	81.2		71.8	0.12
3,4-OCH_2O	66.5	−0.97[e]		

[a] $E_T(30) = 31$. [b] See Figures 1 and 2 for illustration of extrapolations used. [c] Emission from $S_{1,ct}$ in kcal/mol. [d] Emission from $S_{1,np}$ in kcal/mol. [e] Estimated from linear relationship between E_F(ct) and σ_P^+. (See Figure 12).

The Electron-Transfer Reaction, $S_{1,np}$ to $S_{1,ct}$. The detection of both nonplanar and charge-transfer emission from the 2,6-dimethyl-ANS derivative (**2**) in polar solvents suggested that the formation of the charge-transfer state from

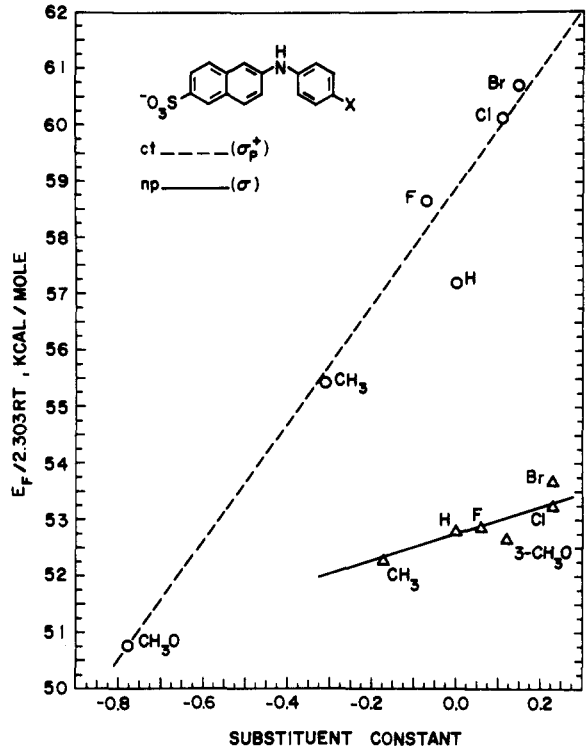

Figure 12. A plot of extrapolated emission maxima (in kcal/mol) vs. substituent constants. Energies corresponding to hydrocarbon solvents were obtained for both $S_{1,np}$ and $S_{1,ct}$ emissions as indicated by the extrapolations shown in Figures 1 and 2 and summarized in Table VIII. The energies were divided by $2.30RT$ in order to scale them appropriately for Hammett substituent constants which are based on equilibrium constants or rate constants. The correlation lines shown yield ρ values of -10.2 for $S_{1,ct}$ vs. σ_p^+ and -2.8 for $S_{1,np}$ vs. σ.

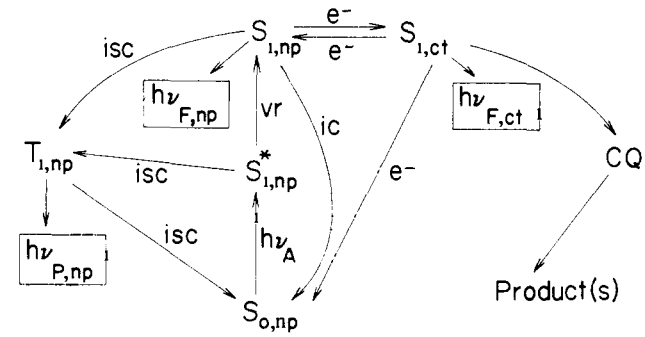

Figure 13. A scheme illustrating the radiative and nonradiative processes for intramolecular donor-acceptor systems as exemplified by 2-*N*-arylamino-6-naphthalenesulfonates (ANS, **1**). Symbols: S, singlet; T, triplet; np, nonplanar relationship of *N*-aryl group to naphthalene ring; ct, charge-transfer; *, nonrelaxed state, used only for vibrational excitation in the scheme; $h\nu_A$, light absorbed; $h\nu_{F,np}$, light emitted by $S_{1,np}$; $h\nu_{F,ct}$, light emitted by $S_{1,ct}$; isc, intersystem crossing between singlet and triplet; ic, internal conversion; e^-, electron-transfer reaction; $h\nu_{P,np}$, light emitted by $T_{1,np}$; CQ, product formed by chemical reaction, thus, chemical quenching; vr, vibrational relaxation.

the nonplanar state was reversible and required favorable geometry for its occurrence. The evidence from absorption spectra had helped to define the equilibrium position of the *N*-aryl group as nonplanar with respect to the naphthalene ring. It appeared likely that charge transfer between the *N*-aryl group and the naphthalene nucleus would be most favorable in a coplanar arrangement of the two rings. Lowering the rate at which a favorable arrangement could be achieved should allow the nonplanar channel for decay to predominate. By raising the viscosity of the solvent around the $S_{1,np}$ molecule, charge transfer would be inhibited. In order to guarantee that the charge-transfer state was possible, the polar solvent glycerol was used. The $E_T(30)$ value of glycerol is 57.0. In dioxane-water mixtures, switchover from nonplanar emission to charge-transfer emission occurs in a solvent with a polarity much lower than that, with $E_T(30) = 52.0$.

The viscous solvent glycerol inhibits the formation of the charge-transfer state for every ANS derivative we have examined, as summarized in Table VI. We have utilized the linear $E_{F,np}$,$E_T(30)$ relationship to estimate the position of emission for glycerol and have found that the predicted and observed values are in good agreement. In addition, emission energies can be measured for the 4-methoxy-ANS and 3,4-methylenedioxy-ANS derivatives in glycerol. The positions of the emissions are consistent with that expected for np emissions.

The Electron-Transfer Reaction, $S_{1,ct}$ to S_0. After absorption spectra of the excited states generated through laser pulses had revealed that triplet was formed only to a limited extent in the solvent-polarity range for which quenching was important, an examination of possible potential-energy curves suggested that return to the ground state via an electron-transfer reaction might be possible. Such a process would: (a) have a rate which was very dependent upon solvent polarity; and (b) occur at a rate much lower than that of the charge-transfer reaction which generated the $S_{1,ct}$ state from the $S_{1,np}$ state. The reason for the latter conclusion is simple; in solvents of certain polarities, a high quantum yield of charge-transfer emission can be observed. Thus, the quenching reaction is much lower in rate than the radiative rate, whereas the rate of formation of the $S_{1,ct}$ state is much higher than the radiative rate ($S_{1,ct}$ and $S_{1,np}$ states have similar lifetimes).[21] In order to inhibit the $S_{1,ct}$ to S_0 reaction without preventing the formation of the $S_{1,ct}$, solvents of high polarity and moderate viscosity were used. 1,2-Ethanediol, 1,2-propanediol, and 1,3-propanediol all behaved in the manner expected; the quantum yields went up sharply, and yet the overall behavior was characteristic of charge-transfer emissions. Emission energies varied very much with solvent polarity. Quantum yields were extremely sensitive to solvent polarity, dropping off very rapidly as water was added since both polarity increase and viscosity decrease favor the quenching reaction. The behavior of the triplet yields as a function of solvent polarity in high polarity solvents proves that intersystem crossing is not the quenching mechanism.

Thus, the phenomenon of quenching of the fluorescence of ANS derivatives in high polarity solvents can be definitively explained in a particularly simple and satisfying way.

General Scheme for Excitation and Decay of ANS Derivatives. The evidence we have described along with other data already published[10] permits the construction of a general scheme for the formation and loss of excited states of 2-*N*-arylamino-6-naphthalenesulfonates. In Figure 13, the initial state is shown as $S_{0,np}$. On absorption of light, a vibrationally excited $S^*_{1,np}$ state is produced. The fastest decay of the $S^*_{1,np}$ state in liquid solution at 25° is via vibrational relaxation to the $S_{1,np}$ state; the isc channel before relaxation is negligible for these conditions but can be detected in glycerol glass at 77 K.[10] The $S_{1,np}$ state has at least four channels through which to decay. The internal conversion (ic) channel is usually unimportant in view of the large energy gap between S_1 and S_0; the laser-pulse results suggest that intersystem crossing (isc) to triplet accounts for a substantial part of the loss of $S_{1,np}$ with the major decay channel being radiative in nonpolar solvents. In more polar solvents, the rate of the electron-transfer reaction which converts $S_{1,np}$ to $S_{1,ct}$ becomes greater than the radiative rate. The electron-transfer reaction is revers-

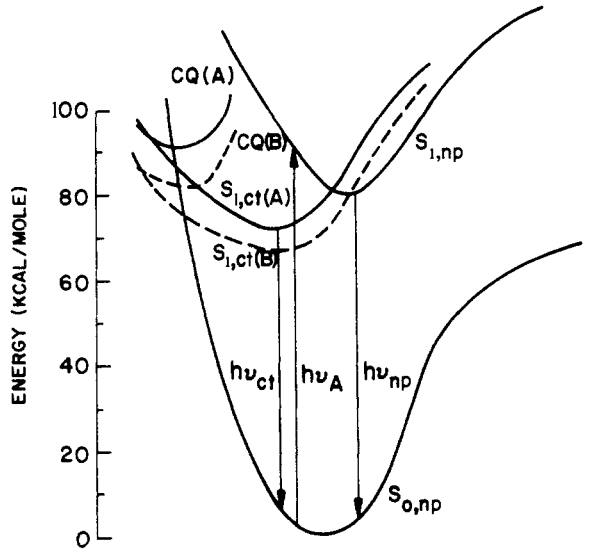

Figure 14. Potential-energy curves for the $S_{0,np}$, $S_{1,np}$, $S_{1,ct}$ states of intramolecular donor-acceptor systems like 2-*N*-arylamino-6-naphthalenesulfonates (**1**). Possible locations for CQ states are also shown. The full line (——) refers to nonpolar solvents, and the dashed line (- - - -) suggests what changes might occur for a shift to polar solvents. The electron-transfer reactions which convert $S_{1,np}$ to $S_{1,ct}$ and $S_{1,ct}$ to $S_{0,np}$ are easy to understand from this set of curves.

ible, and both np and ct emission can be detected in polar solvent solutions of 2,6-dimethyl-ANS (**2**). The $S_{1,ct}$ state can decay through at least four channels. In solvents of intermediate polarity, the major decay channel is radiative. In fluid solvents of high polarity, most of the $S_{1,ct}$ disappears through the electron-transfer reaction which produces a vibrationally excited state of S_0. The electron-transfer reaction which converts $S_{1,ct}$ back to $S_{1,np}$ is probably significant only for a narrow range of solvent polarity [sufficient to change the electron-transfer rate by a factor of 100, roughly speaking equivalent to $\frac{1}{2}\Delta E_T(30)$, as shown for an electron-transfer reaction using $\frac{1}{2}\Delta Z$].[23] The last channel for $S_{1,ct}$ decay is through formation of a chemical quenching product, designated CQ. This represents new absorption seen in laser-pulse experiments. On the basis of the wavelength of maximum absorbance (680 nm) and consideration of reasonable chemical route for the disappearance of $S_{1,ct}$, CQ is tentatively formulated as a dihydrocarbazole derivative (**3**) similar to those postulated by Grellmann et al.[24]

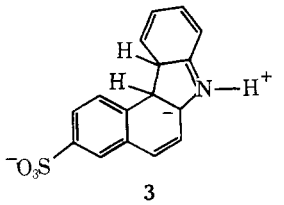

3

However, in contrast to the unstable species reported by Grellmann et al., CQ is formed within less than 20 nsec and does not originate from the triplet state. Further work will be required to establish its structure; CQ represents a minor product probably formed via the $S_{1,ct}$ state. The last group of processes included in the scheme involves the decay of the triplet state. Phosphorescence is easily detected in glycerol glass at 77 K but disappears in fluid solvents. Further investigations on the possible photochemistry of ANS derivatives will be necessary to discover whether or not there are more than the two channels (radiative and intersystem crossing) shown for the $T_{1,np}$ state.

In Figure 14, potential curves are drawn to represent the relationships of the various excited states to the ground state. The effect of solvent on the charge-transfer state ($S_{1,ct}$) level clearly augments the rate of its formation and the rate of its disappearance via electron transfer.

Biological Applications. Our results demonstrate the fragility of the conclusions derived from application of ANS fluorescent probes to biological systems. By raising the viscosity, the quantum yield can be raised to that observed in nonpolar solvents. The emission maximum can also be varied with viscosity since either np or ct emission can be found in polar solvents. The emission maximum, of course, is sensitive to solvent polarity. Given these possible reasons for variations in maximum and quantum yield, it is difficult to obtain specific information on particular biological systems with 2,6-ANS fluorescent probes. We shall try to define the scope for such applications elsewhere.

Conclusions

In addition to significant progress in the understanding of the problem of quenching of ANS fluorescence in polar solvents, a number of excited-state processes have been defined for an intramolecular donor-acceptor system. These results will be applicable to many other intramolecular systems and should be also valuable in understanding excited intermolecular donor-acceptor systems.

The restrictions imposed upon the geometric relationship of the donor and acceptor groups by the one atom connection should permit a differentiation of processes which are ordinarily not susceptible to such dissection. For example, the formation of an exciplex ion pair in polar solvents is often followed by dissociation to ions, which may even occur from the nonrelaxed state of the ion pair.[25] Control of solvent viscosity through temperature or molecular structure permits study of recombination reactions[26] and may even allow direct study of the undissociated ion pair through choices suggested by our work on solvents of intermediate viscosity.

Analysis of excited state phenomena utilizing the effects of solvent polarity [as measured by the empirical parameters $E_T(30)$ and Z] and viscosity on light absorption and emission by the excited states should provide the possibility for a more detailed understanding than heretofore possible.

Experimental Section

Synthesis and Purification. ANS (**1**, X = H) (2-*N*-phenylamino-6-naphthalenesulfonate) sodium salt was synthesized according to the procedure for the magnesium salt,[27] using 18 hr of heating. The reaction mixture was warmed with 10% HCl, and the precipitate was filtered off and recrystallized once from H_2O and twice from 5% aqueous Na_2CO_3.

4-CH_3OANS (1, X = OCH_3). Same procedure was used except with 12 hr of heating. A modification of the Bucherer method[28] was utilized in all other cases, as follows. A solution of 2-amino-6-naphthalenesulfonic acid (1 equiv, 5–10 mmol) (AmNS) and the appropriate aniline (3 equiv, 15–30 mmol) in 33% aqueous $NaHSO_3$ solution (30–50 ml) was refluxed for 1–3 days, the reaction being followed through loss of AmNS by TLC [developer, methanol:benzene (40:60)]. After cooling, the precipitate was filtered off and washed with chloroform (to remove aniline) and water. Pure product was obtained by crystallization (three or four times) from aqueous $NaHSO_3$ (1.4 *M*)-Na_2SO_3 (0.08 *M*), as suggested by Seliskar and Brand.[5] Further notes: 3,4-OCH_2O-ANS, refluxed 3 days, recrystallized three times from H_2O; 3-CH_3O-ANS, refluxed 20 hr, reaction mixture acidified with 10% HCl, precipitate filtered off, recrystallized from 10% NaOH, twice from H_2O.

2,6-DMANS (2-*N*-(2,6-dimethylphenyl)amino-6-naphthalenesulfonate) (2) reaction mxture was refluxed 5 days and recrystallized twice from H_2O.

4-FANS (1, X = F), 4-ClANS (1, X = Cl), and 4-BrANS (1, X = Br) reaction mixtures were refluxed 3 days (Cl), 2 days (Br), and 1 day (F) and treated with hot bisulfite-sulfite solution (50–60 ml/

g) in which the desired product was insoluble, then recrystallized three times from acetone–water (50:50). Column chromatography was used for a number of the compounds, using benzene–methanol in various proportions as eluent. All compounds were dried for at least 3–4 days over P_2O_5 under vacuum. Yields ranged from 10 to 30% except for 2,6-DMANS (0.5%). Purity was established by TLC on silica gel (Eastman 6060) in two different solvent systems, benzene:methanol (60:40) and chloroform:ethanol (60:40). Structures were established by ir, NMR, and uv. Salient characteristics were: ir (NH) 3400 cm^{-1}; NMR (DMSO) aromatic H-naphthalene, aryl [δ 7–8 (m)] NH [δ 8.1–8.6 (1 H, s)] except 2,6-DMANS (**2**) NH [δ 6.2 (1 H, s)]. Groups: 3,4-OCH_2O, δ 5.9 (2 H, s); 2,6-$(CH_3)_2$, δ 2.05 (6 H, s); (in CD_3COCD_3) 4-CH_3, δ 2.3 (3 H, s); 3-CH_3O, δ 3.82 (3 H, s); uv 3 absorption bands (solvents, EtOH, dioxane–water, etc.) representing excitation to S_1, S_2, and S_3 at 360, 320, and 270 nm. Absorption coefficients varied somewhat, to S_1 (4100–6300), to S_2 (15–27,000), and to S_3 (15–30,000). The chief impurity present in most preparations before complete purification is bis(6-sulfonato-2-naphthyl)amine. The structure was established by ir, NMR, uv, and elemental analysis. Purification and spectroscopic properties will be reported separately.

Absorption Spectra. A Cary 17 spectrophotometer was used for all measurements.

Emission Spectra. A Perkin-Elmer Hitachi MPF-3 spectrofluorimeter with a corrected spetra attachment and a digital integrator was used. Quinine sulfate in 0.1 N H_2SO_4 was utilized as a reference standard for quantum yield measurements. Occasional checks of the spectral corrections were run using anthracene in ethanol. Deviations from linearity of response for the MPF-3 were also evaluated and found to be minimal.

Quantum yields were calculated according to the equation[29]

$$(\phi_F)_s = \frac{F_s \epsilon_q C_q (0.55)}{F_q \epsilon_s C_s}$$

with excitation effected at the same wavelength for sample and quinine sulfate. In some cases, as noted in the tables, a correction for refractive index was applied,[30] $(\phi_F)_s$(corrected) = $(\phi_F)_s n^2_D$(solvent)/$n^2_D(H_2O)$. Corrected excitation spectra corresponded to the absorption spectra in all cases. Symbols are defined as follows: F, integrated area under fluorescence curve in arbitrary units; S, sample; q, quinine sulfate; C, concentration; ϵ, absorption coefficient.

Laser Photolysis. Solutions were subjected to laser excitation using the 10 nsec, 10 mJ pulses of an AVCO Everett nitrogen laser. The experimental set-up, including the detection system for nanosecond time resolution have been previously described.[31]

Solutions. A stock solution of ANS derivative (10^{-5} M) in 98% dioxane–water (for dioxane–water mixtures) or in pure solvent (glycerol, 1,2-ethanediol, 1,2-propanediol, 1,3-propanediol) was prepared. An aliquot (0.2 ml) of stock solution was placed in the fluorescence cell and additional solvent (of specific volume ratios) (3.0 ml) added; final compositions are recorded in the tables. After thorough mixing, the solutions (ca. 10^{-6} M) were placed in the MPF-3. Temperature effects were determined to be very small over the range of interest (24 ± 2°), and spectra were thus recorded at ambient temperature as measured in the compartment.

Solvents. Dioxane was either Spectroscopic Grade (Fluka) or carefully purified according to the procedure described by Riddick and Bunger[32] with purity established by lack of absorption above 220 nm (OD under 0.6 for pure solvent). Glycerol (for fluorescence microscopy) (E. Merck, Darmstadt) was handled in a glove bag under dry nitrogen. 1,2-Ethanediol was supplied by Merck (zur Analyse). 1,2-Propanediol and 1,3-propanediol were reagent grade materials supplied by Fluka. None of the solvents had fluorescent impurities.

Plotting of Data. Maxima were carefully read from the corrected emission curves. Together with quantum yield data, these were stored on magnetic cards through a Hewlett-Packard 9810 calculator. The data were plotted from the cards with a Hewlett-Packard 9862 X-Y plotter. Not only did this procedure minimize human error in plotting hundreds of similar data points, but comparison of different measurements was made extremely simple through replotting of the desired data on a single chart. The calculator-plotter combination was also used to resolve the emission curves for DMANS in polar solvents. The observed emission curve was recorded.[33] The emission curve in 99% dioxane (pure np emission) was adjusted so that the intensity of the maximum matched that of the observed curve, and each intensity was multiplied by the adjustment factor. The latter curve was subtracted from the observed curve to yield the curve for the charge-transfer emission. The ct emissions obtained by this route are [% dioxane-water, $E_T(30)$ value, $\lambda_{max}(\phi_F)$]: 43.2, 54.9, 450 (~0.025); 34.4, 56.5, 452 (0.021); 29.7, 57.2, 456.5 (0.015); 26.3, 57.9, 458 (0.014); 20.3, 58.7, 461 (0.012); 10.9, 60.9, 470 (0.004). The slope of the plot of emission energies against $E_T(30)$ is 0.62.

Solvent Polarity Measurements. Pyridinium phenol betaine 30 was kindly supplied by Professor K. Dimroth. The compound was dissolved in the solvent under consideration and the absorption maximum carefully measured. The position of the maximum, expressed as kcal/mol, is the $E_T(30)$ value. Dioxane–water $E_T(30)$ values were interpolated from those reported by Reichardt and Dimroth.[14]

Acknowledgment. We are grateful for helpful discussion with Professor J. Jortner. Support of the United States-Israel Binational Science Foundation in obtaining equipment is appreciated.

References and Notes

(1) (a) Tel-Aviv University; (b) State University of New York; (c) Hebrew University.
(2) (a) G. Weber and D. J. R. Laurence, *Biochem. J.*, **56**, xxxi (1954); (b) L. Stryer, *J. Mol. Biol.*, **13**, 482 (1965); see also *Science*, **162**, 526 (1968).
(3) W. O. McClure and G. M. Edelman, *Biochemistry*, **5**, 1908 (1966).
(4) D. C. Turner and L. Brand, *Biochemistry*, **7**, 3381 (1968); see also L. Brand and J. R. Gohlke, *Annu. Rev. Biochem.*, **41**, 843 (1972).
(5) C. J. Seliskar and L. Brand, *J. Am. Chem. Soc.*, **93**, 5405, 5414 (1971).
(6) E. . Kosower and K. Tanizawa, *Chem. Phys. Lett.*, **16**, 419 (1972).
(7a) See, for example, A. Beens, H. Knibbe, and A. Weller, *J. Chem. Phys.*, **47**, 1183 (1967); (b) E. A. Chandross and H. T. Thomas, *Chem. Phys. Lett.*, **9**, 393 (1971); (c) T. Okada, T. Fujita, M. Kubota, S. Masaki, N. Mataga, R. Ide, Y. Sakata, and S. Misumi, ibid., **14**, 563 (1972).
(8) J. R. Huber and J. E. Adams, *Ber. Bunsenges. Phys. Chem.*, **78**, 217 (1974).
(9) Two conformations, the helical and the perpendicular, have been discussed for Ar_2ZXY systems by D. Gust and K. Mislow, *J. Am. Chem. Soc.*, **95**, 1535 (1973). For many purposes, they point out that the perpendicular conformation can be considered as a time average of two helical conformations. However, the time scale for the averaging process clearly approaches that of the radiative process in solutions of suitable viscosity (more accurately, appropriate microviscosity) so that each rotational state may have to be considered as a separate species with respect to the ANS excited state processes.
(10) E. M. Kosower Ind H. Dodiuk, *Chem. Phys. Lett.*, **26**, 545 (1974).
(11) E. M. Kosower, "An Introduction to Physical Organic Chemistry", Wiley, New York, N.Y., 1968.
(12) N. Mataga, Y. Kaifu, and M. Koizumi, *Bull. Chem. Soc. Jpn.*, **28**, 690 (1955).
(13) E. Lippert, *Z. Naturforsch. Teil A*, **10**, 541 (1955).
(14) K. Dimroth and Ch. Reichardt, *Justus Liebigs Ann. Chem.*, **663**, 1 (1963); Ch. Reichardt and K. Dimroth, *Fortsch. Chem. Forsch.*, **11**, 1 (1968).
(15) The choice of reference system for linear free-energy relationships is discussed in ref 11.
(16) We are grateful to Professor K. Dimroth for supplying us with a sample of the betaine-30 used for the measurements (see ref 14). Many of the results have been communicated. E. M. Kosower and H. Dodiuk, *J. Am. Chem. Soc.*, **96**, 6195 (1974).
(17) J. Jortner, *Pure Appl. Chem.*, **27**, 389 (1971).
(18) M. Ottolenghi, *Acc. Chem. Res.*, **6**, 153 (1973).
(19) N. Orbach, R. Potashnik, and M. Ottolenghi, *J. Phys. Chem.*, **76**, 1133 (1972).
(20) N. Orbach, J. Novros, and M. Ottolenghi, *J. Phys. Chem.*, **77**, 2831 (1973).
(21) Lifetimes for ANS derivatives are approximately 12 nsec by the single photon counting technique.[22] The substituent and solvent dependences of the lifetimes will be reported separately.
(22) Lifetimes for the $S_{1,ct}$ states are slightly longer than those for the $S_{1,np}$ states, but the indicated order of magnitude applies to both states.
(23) M. Mohammad and E. M. Kosower, *J. Am. Chem. Soc.*, **93**, 2713 (1971).
(24) K. H. Grellmann, E. W. Forster, and H. Linschitz, *J. Am. Chem. Soc.*, **95**, 3108 (1973). The difference in lifetimes may be due to the difference in N substitution (N–H in **3** vs. N–CH_3).
(25) M. Shimada, M. Masuhara, and N. Mataga, *Bull. Chem. Soc. Jpn.*, **46**, 1903 (1973).
(26) M. Ottolenghi and N. Orbach, Proceedings of International Exciplex Conference, London, Ontario, Canada, May 1974.
(27) R. P. Cory, R. R. Becker, R. Rosenbluth, and I. Isenberg, *J. Am. Chem. Soc.*, **90**, 1643 (1968).
(28) H. Bucherer and A. Stohmann, *Chem. Zentralbl.*, **75**, 1012 (1904).

(29) C. A. Parker and W. T. Rees, *Analyst (London)*, **85**, 587 (1960).
(30) J. N. Demas and G. A. Crosby, *J. Phys. Chem.*, **75**, 991 (1971).
(31) C. R. Goldschmidt, M. Ottolenghi, and G. Stein, *Isr. J. Chem.*, **8**, 29 (1970).
(32) J. A. Riddick and W. B. Bunger, "Organic Solvents" (Techniques of Chemistry Series), Vol. 2, A. Weisberger, Ed., Wiley, New York, N.Y., 1970, p 706.
(33) Appropriate multiplication and division procedures made it possible to store and recover 3 numbers per register. The limited capacity (111 registers) of the calculator is just sufficient for the task.

Solution Photochemistry. XIII.[1] Hydrogen Abstraction Reactions Proceeding through Five-Membered Transition States. Mechanistic Studies Indicating Conformational Control[2]

John R. Scheffer,* Kuldip S. Bhandari, Rudolf E. Gayler,[3a] and Rockford A. Wostradowski[3b]

Contribution from the Department of Chemistry, University of British Columbia, Vancouver, British Columbia, V6T 1W5, Canada. *Received March 23, 1974*

Abstract: The photochemistry of a variety of substituted acyclic 1,3-diene-*p*-quinone Diels–Alder adducts has been investigated. Irradiation of these systems in their long wavelength absorption bands leads to novel tricyclic ring systems in moderate to good yields. Derivatives of the following basic ring systems are produced in this way: tricyclo[4.4.0.$0^{2,8}$]decane, tricyclo[4.4.0.$0^{2,9}$]decane, tricyclo[4.4.0.$0^{3,9}$]decane, and tricyclo[5.3.1.$0^{2,7}$]undecane. The ratio in which the products are formed is generally solvent dependent. Deuterium labeling studies indicate that, in most instances, the major primary process in the photochemistry of substituted butadiene-*p*-benzoquinone Diels–Alder adducts consists of abstraction of a β-hydrogen atom by the excited carbonyl oxygen. The products are then derived from carbon–carbon bond formation in the bis(allylic) radical so produced. For unsymmetrical adducts, in which the β-hydrogen atoms are nonequivalent, abstraction occurs in accord with expectations based on the formation of the more stable diradical intermediate. However, exceptions to these reactivity patterns are found when the adducts possess either (a) C_5 and/or C_8 substituents (R = Me or Ph) or (b) bridgehead methyl substituents. In the former case, exclusive γ-hydrogen abstraction by oxygen is observed when R = Me, and when R = Ph the molecule is photochemically inert. In the case of the unsymmetrical piperylene–benzoquinone adduct (R = Me, R′ = H), β-hydrogen abstraction competes only poorly with γ-hydrogen abstraction. On the other hand, bridgehead methyl substitution brings about partial suppression of the β-hydrogen abstraction reaction in favor of a process tentatively concluded to involve γ-hydrogen abstraction by excited enone carbon. In general, these reactivity differences are interpreted as being due to the effects of the substituents on the ground state conformations of the basic tetrahydro-1,4-naphthoquinone ring system involved. The tricyclic photoproducts found in this study are nearly all thermally and/or photochemically labile and undergo unusual sigmatropic rearrangements whose mechanisms are discussed. In addition, the resemblance of the various tricyclic photoproducts formed in these reactions to naturally occurring sesquiterpenes is noted, and, finally, possible explanations are advanced for the variations in photoproduct ratios with solvent.

The endo Diels–Alder adducts of *p*-benzoquinone with cyclic 1,3-dienes are well known[4] to give cage products upon photolysis via internal 2 + 2 cycloaddition. However, prior to our work, no determined effort had been made to study the photochemistry of Diels–Alder adducts of *p*-benzoquinone with *acyclic* 1,3-dienes.[5] We report in this paper that these adducts, possessing the tetrahydro-1,4-naphthoquinone ring system, do not undergo intramolecular cycloaddition upon photolysis but rather take part in a remarkably general rearrangement leading to novel tricyclic ring systems. In addition, we report experiments which establish that these rearrangements are initiated by the rarely observed process of intramolecular β-hydrogen atom abstraction, i.e., abstraction through a five-membered transition state.

Scheme I

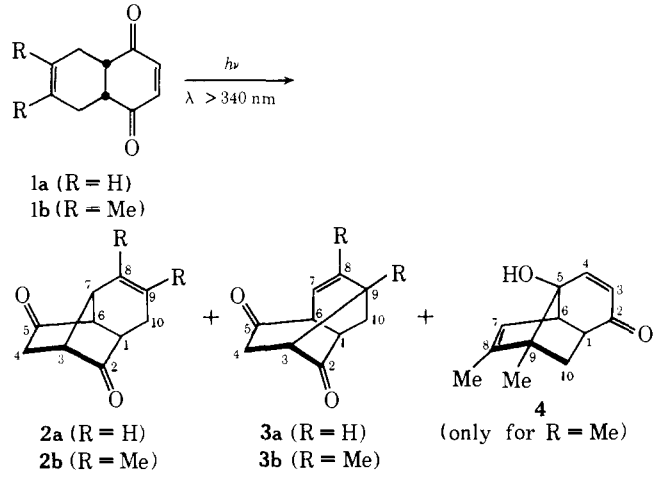

Results and Discussion

Photolysis of Diels–Alder Adducts of *p*-Benzoquinone with Butadiene (1a) and 2,3-Dimethylbutadiene (1b). In agreement with previous reports,[5] photolysis of the 1,3-butadiene-*p*-benzoquinone Diels–Alder adduct **1a** (Scheme I) through Pyrex in a variety of solvents led only to intractable polymeric material. However, selective n → π^* excitation of **1a** in benzene (uv_{max} 370 nm, ϵ 67)[6] using a Corning 7380 glass filter (transmitting $\lambda \geq 340$ nm) gave material whose crude ir spectrum showed weak absorptions in the 5.7 μ region indicating the presence of the cyclopentanone chromophore. This material was freed from polymer by passage through a short chromatography column containing neutral alumina (chloroform eluent) and the resulting mixture analyzed by GLPC which showed the presence of two